Supplement of Solid Earth, 10, 1685–1705, 2019
https://doi.org/10.5194/se-10-1685-2019-supplement

Solid Earth Open Access EGU

Supplement of

Subsurface characterization of a quick-clay vulnerable area using near-surface geophysics and hydrological modelling

Silvia Salas-Romero et al.

Correspondence to: Silvia Salas-Romero (silvia.salas_romero@geo.uu.se)

Table S1. Main processing steps applied to both land and river seismic data.

Step	Parameters
Land reflection seismic data	
1	Read 0.5 s SEG-Y data
2	Zero-time correction
3	Vertical shot stacking (lines 2b, 6 and 7)
4	Merge lines from 2011 and 2013 (lines 2 and 2b, and lines 5 and 5b)
5	Extract and apply geometry: CDP spacing 2 m and 10 m (line 5–5b wireless)
6	Trace editing
7	First break picking: automatic picking and manually corrected
8	Elevation static corrections: datum 20-25 m and replacement velocity 1500 ms^{-1}
9	*f–k* filter (line 5–5b wireless)
10	Wiener deconvolution: gap 10-15 ms
11	Band-pass filter: 40-60-200-250 Hz (lines 6 and 7), 40-60-180-200 Hz (line 2–2b), 70-80-260-280 Hz (line 5–5b cabled) and 30-60-180-200 Hz (line 5–5b wireless)
12	Spectral whitening: 70-80-180-200 Hz (line 5–5b cabled) and 70-80-200-220 Hz (line 5–5b wireless)
13	Top mute using first breaks
14	Surgical mute (line 5–5b wireless)
15	Airwave mute
16	AGC: 70-500 ms
17	Velocity analysis
18	Residual static corrections (lines 6 and 7)

19	Normal moveout (NMO) corrections: 50-150 % stretch mute
20	Stack
21	Band-pass filter: 20-40-150-170 Hz (lines 6 and 7), 50-60-150-170 Hz (line 2–2b) and 30-40-110-130 Hz (line5–5b wireless)
22	Post-stack deconvolution (line 5–5b wireless)
23	*f–x* deconvolution
24	Trace balance
25	*f–k* filter (lines 6 and 7)
26	Time-to-depth conversion using constant velocity of 1500 ms^{-1}

River reflection seismic data

1	Read 0.2 s SEG-Y data
2	Apply marine geometry
3	Wiener deconvolution: gap 2-6 ms
4	AGC: 100 ms
5	NMO corrections: 30 % stretch mute
6	Stack
7	Post-stack deconvolution
8	Top mute
6	*f–x* deconvolution
7	Trace balance
8	Time-to-depth conversion using constant velocity of 1500 ms^{-1}

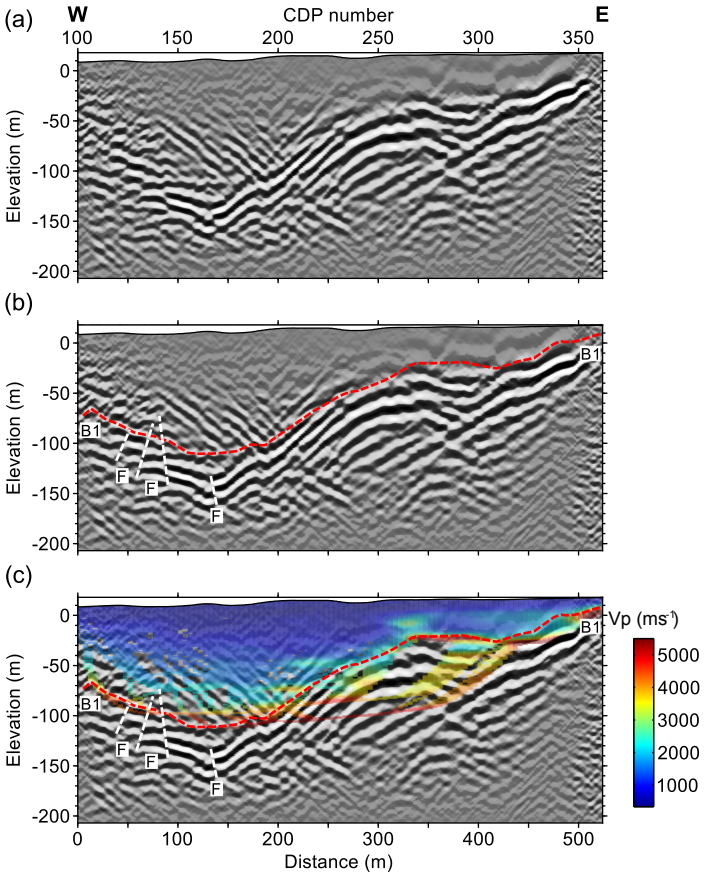

Figure S1. Onshore datasets for line 6. **(a)** Reflection seismic processing results. **(b)** Interpreted seismic section, with only a major reflection, B1, identified from the bedrock (dashed red line). At different positions, several fractured or disturbed materials (F) are also delineated using a dashed white line. **(c)** P-wave refraction tomography model (Wang et al., 2016) superimposed on the interpreted seismic section illustrating consistency between the two independent methods.

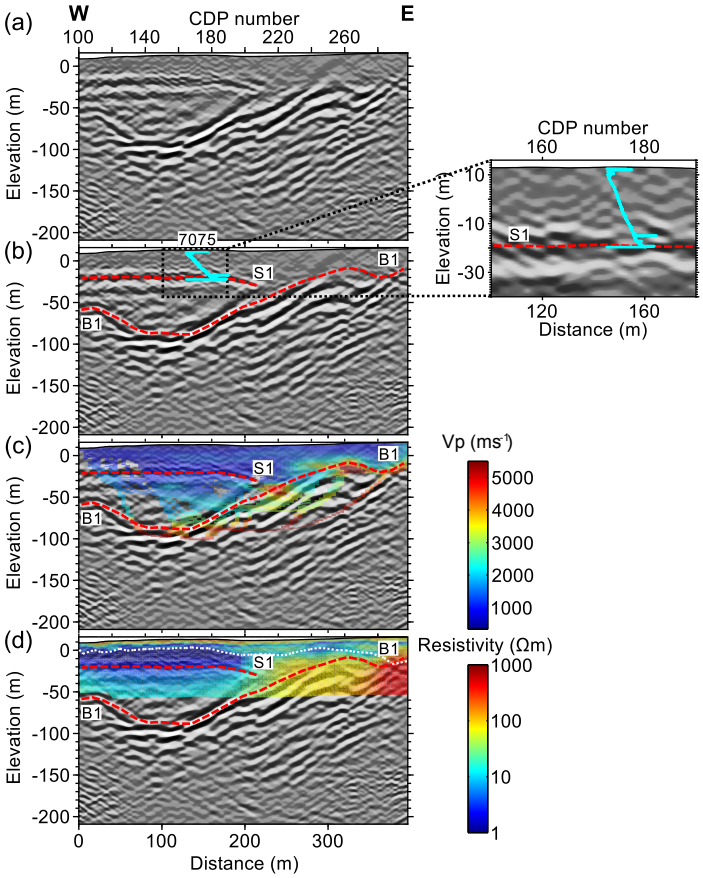

Figure S2. Onshore datasets for line 7. **(a)** Reflection seismic processing results. **(b)** Interpreted seismic section including total sounding data (BGA, 2018) from borehole 7075 (ranging from 0 to 14 kN) in blue. S1 (top of the coarse-grained materials) and B1 (top of the bedrock) represented by dashed red lines. **(c)** P-wave refraction tomography model (Wang et al., 2016) superimposed on the interpreted seismic section. **(d)** RMT resistivity results (Wang et al., 2016) superimposed on the interpreted seismic section. The dashed white line indicates the depth above which the results are considered of higher confidence.

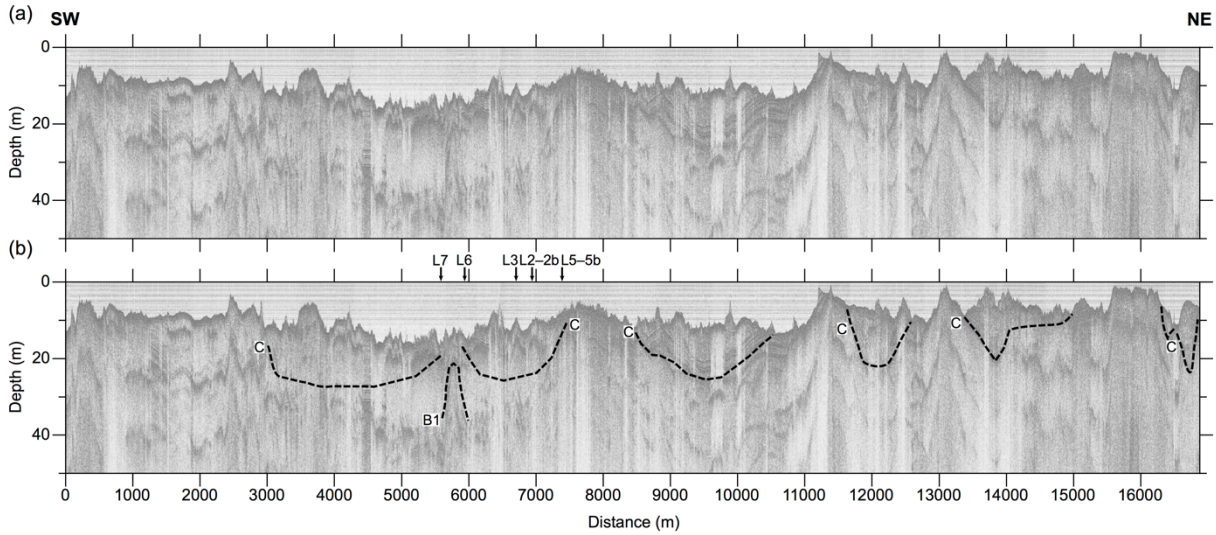

Figure S3. Processing results of the single-channel (3.5 kHz echo sounder) river seismic data (© SGU). **(a)** Seismic processed section. **(b)** Interpreted seismic section. C (filled channels) and B1 (top of the bedrock) represented by dashed black lines. The positions of the land seismic lines that intersect this line are indicated on top of the section. Scale 1H:57V.

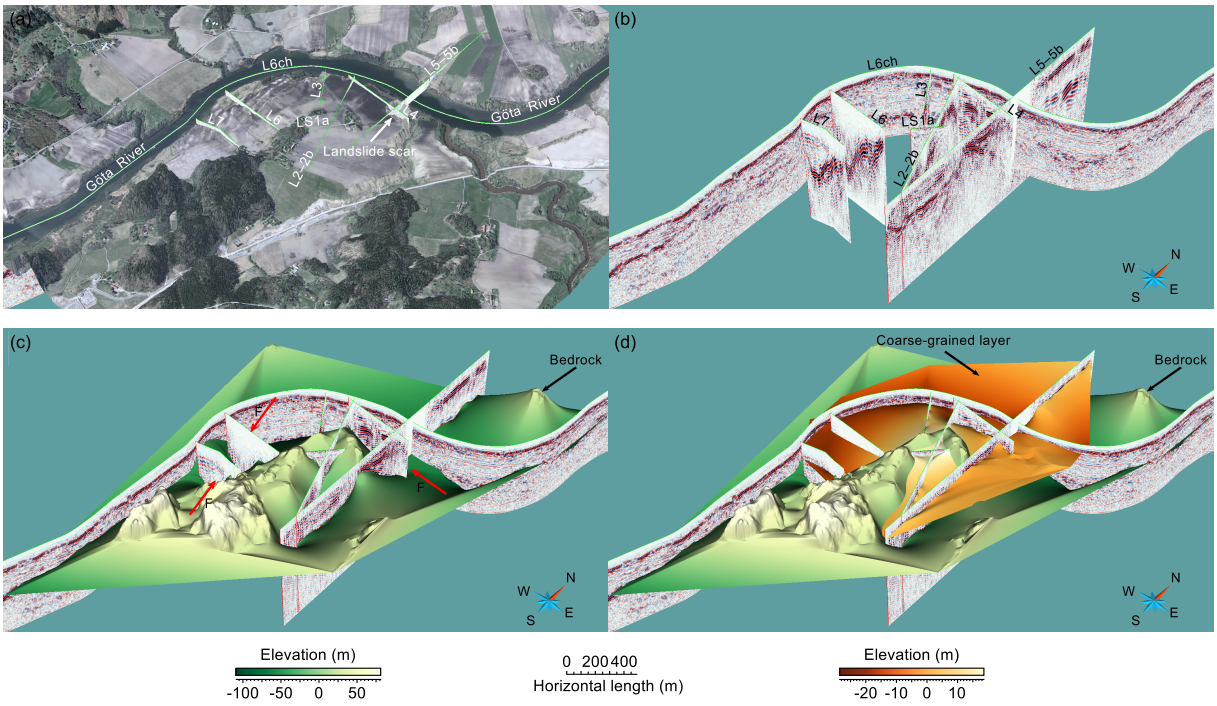

Figure S4. 3-D modelling of the subsurface at the survey site (south view). **(a)** Aerial photo projected on the lidar elevation surface (© Lantmäteriet) of the study area with the positions of the land and river seismic lines along the Göta River. **(b)** 3-D view of the land and river seismic processed lines. **(c)** Elevation of the bedrock surface (F indicates the position of interpreted faults, also observed in Fig. 2a). **(d)** Elevation of the coarse-grained layer and bedrock surfaces.

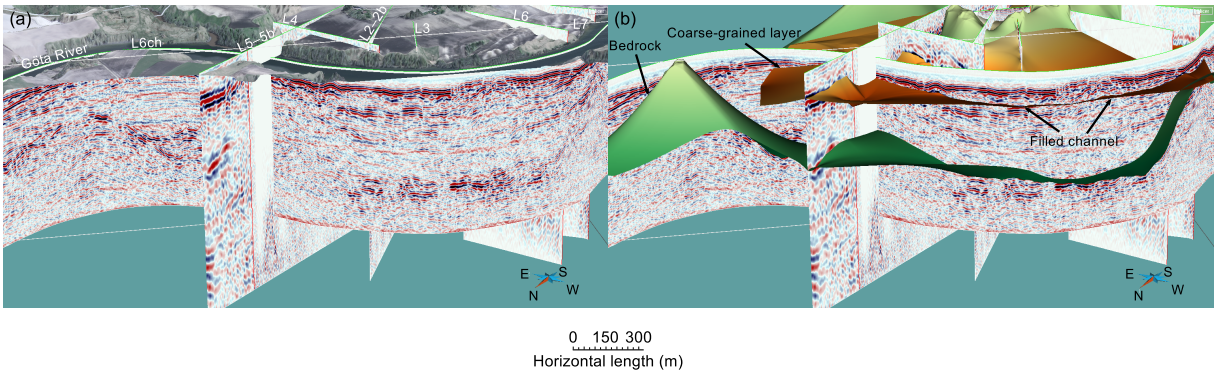

Figure S5. 3-D views of the seismic data and key surfaces in the study area. **(a)** Aerial photo projected on the lidar elevation surface (© Lantmäteriet) with the positions of the land and river seismic lines along the Göta River. **(b)** Elevation of the coarse-grained layer and bedrock surfaces. Note the coincidence of the coarse-grained layer surface with the delineation of one of the filled channels (see Figs. S3, 7 and 8). Observe also the undulated bedrock surface between lines 6 and 7 located on the right side of the figure. See elevation values for both surfaces in Fig. S4.

Table S2. Hydrological measurements in or near the coarse-grained layer (BGA, 2018; Salas-Romero et al., 2016).

Name	X (m)	Y (m)	Pressure (m)	Z (m)	Vertical hydraulic gradient at the coarse-grained layer	Notes	In the model domain
BH1	331767.66	6454139.96	23	-10	–	Winter	Yes
BH2	331827.11	6454582.84	11	??	–	Winter	Yes
BH3	331991.53	6454378.35	14.5	-20	–	Winter	Yes
7052	332189.98	6454719.86	9.4	-21	Up	Artesian	No
7053	332198	6454690.07	8.1	-10.4	Up	–	No
7054	332221.03	6454609.99	8.3	-9.1	Up	–	No
7063	331583.73	6454638.19	7.7	-21.9	Up	–	Yes
7064	331595.99	6454609.98	10.1	-12.2	Up	Seasonally artesian	Yes
7065	331619.02	6454550	11.2	-10.6	–	–	Yes
7073	331051.03	6453638.89	10.3	-26.2	Up	Artesian	No
7075	331179.6	6453643.24	12	-24.8	Up	–	No

Table S3. Hydrological measurements above the coarse-grained layer (BGA, 2018).

Name	X (m)	Y (m)	Pressure (m)	Z (m)
7052	332189.98	6454719.86	7.1	6
7052	332189.98	6454719.86	7.4	1
7052	332189.98	6454719.86	7.44	-2.4
7053	332198	6454690.07	16.2	16.6
7053	332198	6454690.07	14.1	11.6
7053	332198	6454690.07	11.3	4.6
7053	332198	6454690.07	7.7	-3
7054	332221.03	6454609.99	19.9	17.9
7054	332221.03	6454609.99	19.4	12.9
7054	332221.03	6454609.99	15.9	5.9
7054	332221.03	6454609.99	7.5	-3.7
7063	331583.73	6454638.19	8.2	5.1
7063	331583.73	6454638.19	6.9	0.1
7063	331583.73	6454638.19	7.3	-6.9
7064	331595.99	6454609.98	16.3	13.8
7064	331595.99	6454609.98	15	9.8
7064	331595.99	6454609.98	12.8	2.8
7064	331595.99	6454609.98	10	-12.2
7065	331619.02	6454550	18.4	15.4
7065	331619.02	6454550	17.7	11.4

7073	331051.03	6453638.89	7.7	3.8
7073	331051.03	6453638.89	8.2	-0.2
7073	331051.03	6453638.89	9.6	-7.2
7075	331179.6	6453643.24	11.9	9.3
7075	331179.6	6453643.24	12.8	5.3
7075	331179.6	6453643.24	12.6	-1.7
7056	332113.11	6454510.08	20.2	19.3
7060	331908.12	6454669.9	16.4	15.6
7069	331408	6454520	15.4	13.3